ISSN: 0976-9102 (ONLINE)
DOI: 10.21917/ijivp.2025.0496

ENHANCED ENSEMBLE SEGMENTATION OF LUNG CHEST X-RAY IMAGES BY DENOISING AUTOENCODER AND CLAHE

V. Thamilarasi[1], A. Asaithambi[2] and R. Roselin[3]
[1,3]Department of Computer Science, Sri Sarada College for Women, India
[2]Department of Computer Science, Florida Polytechnic University, United States of America

Abstract

This article describes a novel ensemble approach to achieve high quality segmentation of Chest X-Ray (CXR) images. Specifically, the Japan Society of Radiological Technology (JSRT) dataset consisting of 247 CXR images has been used to study the effectiveness of this approach. The study has been carried out in three phases: preprocessing, segmentation, and validation by classification. The novelty of the study comes from combining a Denoising Autoencoder with Contrast Limited Adaptive Histogram Equalization (CLAHE) for preprocessing; an ensemble method that combines Canny edge detection with morphology, Otsu thresholding, automatic thresholding, and granule segmentation for segmentation; and the Gray-Level Co-occurrence Matrix (GLCM) for feature extraction to aid in classification. The quality of classification of lung CXR images as nodules vs. non-nodules, and malignant vs. benign, using this unique combination of various standard approaches for segmentation coupled with a variety of classifiers such as Random Forest, Decision Tree, Naive Bayes, Support Vector Machine (SVM), Logistic regression, K-Nearest Neighbor (KNN), and XGBoost has been validated with Receiver Operating Characteristic (ROC) curves. This study attains high accuracy of 97.67% for enhanced ensemble segmentation and accuracy of 98.93% for nodule/nonnodule classification and 99.18% accuracy for malignant/benign classification with SVM.

Keywords:

Medical Image Analysis, Chest X-Ray Images, Segmentation, Classification, Nodule, Non-Nodule, Thresholding, Granule

1. INTRODUCTION

Medical image analysis using machine learning has become an increasingly important area of research in recent years due to its potential for helping physicians identify and treat diseases in the internal organs of the human body. In particular, the presence of several organs in the chest area makes the analysis of Chest X-Ray (CXR) images more challenging than the analysis of MRIs and CT scans.

Under normal circumstances, the cells in the human body divide, grow, and die to provide room for new cells. This systematic phenomenon sometimes breaks down and some cells tend to grow uncontrollably and spread, affecting the surrounding tissue. Such growth of cells could result in what is called a tumor. A tumor is a lump of tissue, which can be cancerous (malignant), or non-cancerous (benign). A benign tumor does not spread throughout the body, but a malignant tumor could migrate to different parts of the body, disturb the growth of adjacent cells, and hence be harmful. As the place of growth determines the nature of the cancer, most of the time, the patient may already be in critical condition when the cancer is detected. In particular, the detection of cancer in the lungs requires keeping track of growing cells that may start as small-sized nodules and enlarge into tumors with the potential of becoming cancerous. Thus, cancer detection must be carried out in two steps: first, the detection or classification of cell growth as nodules and non-nodules, and second the classification of nodules as malignant or benign.

Of all the CXR images, lung images are the most difficult to analyze especially in the presence of diseases as the shape of the lungs could change or the areas surrounding the lungs might have been affected. Image segmentation is therefore a crucial first step in the analysis of CXR images for detecting lung cancer. Efficient and accurate methods for CXR image segmentation are needed to help physicians treat patients properly and in a timely manner. Presented in this article is a novel ensemble approach for segmentation of CXR images of the lungs, followed by their classification into nodules and non-nodules first, and then the classification as malignant or benign. The rest of this article is organized as follows. Section 2 discusses related work and highlights the significance of the present work. Section 3 describes the methodology in brief. Section 4 presents the findings from the investigation. Section 5 includes some concluding remarks along with recommendations and suggestions for future work.

2. RELATED WORK

In this section, we explore and describe previous works reported in the literature that are related to image segmentation and classification.

In relation to image segmentation and thresholding, Priya, Agrawal, and Rana [1] investigate the Otsu [2], Tsallis [3], and Kapur [4] entropy threshold methods, propose a multilevel threshold technique based on fusion, achieve good segmentation accuracy on MRI datasets. Ramesh, Kumar, Swapna, Datta, and Rajest [5] provide a review of a variety of image segmentation approaches including region growing, region split and merge, watershed, clustering, edge detection, and model-based approaches including the Lattice Bolzman (LB) method. Liu et al. [6] carry out karyotype analysis using the chromosome image segmentation and the Otsu region-growing algorithm. Fang [7] proposes combining fuzzy theory with thresholding for image segmentation. This work determines the threshold by maximum inter class variance method; the gray and spatial similarity between neighboring pixels by weighted value method; and the membership function of the target and the background by normalized synthesis. Xinying, Zhijun, Jun, and Keming [8] introduces the idea of combining granular hierarchy with immunological mechanisms and develops the robust granular immune algorithm (GIA) for image segmentation. The main advantage of GIA is that it is capable of global searching without being trapped into local optima and it can be made faster through parallel implementations. Liao et al. [9] improve upon the Otsu thresholding method [2] obtain a fast, recursive algorithm for one-

dimensional multi-level thresholding. The speed and efficiency of this method is achieved by modifying between class variance formulas to a form, which also makes this approach suitable for other thresholding mechanisms such as entropic thresholding and correlation measures. He et al. [10] propose a generalized 2D histogram that uses the Renyi entropy [11] to calculate the threshold, which improves the image segmentation performance. They demonstrate that their results are superior to those obtained using seven previously developed approaches of 1D KSW, 2D KSW, 2D Renyi, 2D Tsallis, GLSC, 2D-D, and GLCM. Another novel entropy has been introduced in Nie, Zhang, Li, and Ding [12]. Thresholding based on this entropy led to more accurate results than previous state of the art methods on non-destructive testing images, infrared images, and real images.

In relation to machine learning algorithms for classification, we begin by describing the work of Raoof et al. [13], which examines the origins, variations, and global effects of cancer; discusses several machine learning algorithms and their applications for disease diagnosis; and offers a method for choosing an appropriate machine learning algorithm from among several such as support vector machines, artificial neural networks, recurrent neural networks, just to name a few. Another survey that examines the relationship between different machine learning algorithms and the approaches they provide to solve realworld problems is provided by Sarker [14]. The realworld applications this survey considers include smart cities, cybersecurity, healthcare, e-commerce, agriculture, and so on. This work also offers technical advice to researchers, business professionals, and those who wish to solve real-world problems through machine learning. Pratondo, Chui, and Ong [15] present a novel method to improve the accuracy of support vector machines and K-nearest neighbors' approach by using the Chan-Vese algorithm [16]. Wang et al. [17] experiment with 1102 CXR images for Covid-19 analysis by combining deep features with machine learning classification and achieve a 99.33% accuracy with an Xception+SVM model, which is a 2.58% improvement over the 96.75% accuracy achieved with Xception alone. To identify the severity of Covid-19 through CT images, Khan, Garner, Rocca, Salehi, and Duncan [18] use a semi-automatic threshold approach to segment the picture based on region of interest (ROI). They achieve a precision score of 47.59% and a specific score of 98.49%, which are both improvements over other Covid-19 ROI segmentation methods. Muhamedyev, Yakunin, Iskakov, Sainova, Abdilmanova, and Kuchin [19] perform a comparative study to explain how well different learning algorithms are learn by examining the overfitting, perfect case, and underfitting learning rates of algorithms such as the Naive Bayes method, K-nearest neighbors, and neural networks. The experiments of this study use the log data of the from the Kazakhstani uranium reserves at Inkai. Another comparative study of classification algorithms in machine learning is by Savchuk and Doroshenko [20], which investigates the effectiveness of Support Vector Machines, Extra Trees, Random Forests, Decision Trees, Logistic Regression, MLP classifier, Gradient Boosting, and Naive Bayes Classifier. The metrics of accuracy, precision, recall, F1-measure, and ROC are used for the comparison. Through a survey of feature extraction techniques, Salau and Jain [21] conclude that the most unique Gray Level Difference Statistics (GLDS) features that can be extracted are mean, homogeneity, entropy, energy, and contrast; they also conclude that feature extraction techniques can be used in a variety of applications.

The present study differs from the previous studies as it is focused on an ensemble approach for segmentation of CXR images, to help achieve the goal of classifying the images as nodules or non-nodules, and malignant or benign. This study is an extension of the works reported in [2] [22-25]. The study has been carried out in several phases, as depicted in Fig.1, the workflow for the analysis in the study.

In the first phase, a denoising autoencoder and contrast-limited adaptive histogram equalization (CLAHE) is used for preprocessing, which is the first major contribution of this study.

In the second phase, an ensemble approach for segmentation is used with the goal of increasing segmentation accuracy by combining the four different segmentation approaches of Canny edge detection with morphology, Otsu thresholding, automatic thresholding, and granule-based segmentation. This approach leads to a much higher accuracy when compared to the accuracy achieved by methods reported previously in the literature. This ensemble approach is the second major contribution of this study.

The next phase is feature extraction, which leads to the extraction of features such as contrast, correlation, energy, entropy, homogeneity, mean, and standard deviation are extracted using the GrayLevel Co-occurrence Matrix (GLCM) approach, which is the third major contribution of the present study.

The last phase of the study is classification, or the process of labelling the given set of CXR images of tumors into the classes of nodules and non-nodules, and then classifying them further as malignant and benign, using several machine learning algorithms such as Random Forests, Decision Trees, Naive Bayes, Support Vector Machine (SVM), Logistic regression, K-Nearest Neighbour (KNN), and XGBoost. The performance of the suggested techniques has been evaluated using the metrics of sensitivity, specificity, accuracy, and dice similarity.

Fig.1. Workflow for the Analysis of Chest X-Ray Images

3. METHODOLOGY

The study uses the JSRT database, jointly developed by the Japanese Society of Radiological Technology (JSRT) and the Japanese Radiological Society (JRS). This database consists of a total of 247 images, of which 154 are nodule images and 93 are

non-nodule images. A denoising autoencoder and context limited adaptive histogram equalization are used for preprocessing these images. An ensemble of four robust segmentation methods is used to achieve a high segmentation accuracy. The segmentation results are evaluated. GLCM is used for feature extraction. Based on these features extracted using GLCM, several machine learning classification algorithms are employed, and the classification results are evaluated. The JSRT images are available at a size of 2048 × 2048 pixels. Any size changes of the images have been carried out using the Image J software tool.

3.1 IMAGE PREPROCESSING

The entire manuscript should be in Times New Roman. Other font types may be used if required only for special purposes. Refer to Table.1 for font sizes.

3.1.1 Denoising Autoencoder (DAE):

An autoencoder, commonly used for dimension reduction, is a neural network that is used to recreate the features of an input image in its output. However, to avoid creating an output that is identical to the noisy input, a denoising autoencoder is used. A denoising autoencoder typically consists of three parts: the encoder, compressed data, and the decoder.

The encoder converts an input image into a compressed form by masking some pixel values and adding noise to the image; the decoder then removes the noise to recover the original input image. A schematic of the denoising autoencoder is shown on Fig.2.

In Fig.2, the leftmost yellow column represents the collection of pixels x in the input image. After masking some pixels in x, as denoted by the $\otimes$, this collection becomes $x^{\sim}$, the second column from the left in Fig.2. The denoising autoencoder receives $x^{\sim}$ with some added noise as input; this input is passed through the encoder network E, yielding the compressed form x' of $x^{\sim}$; finally, the decoder network D takes the noisy x' and denoises it to reconstruct the image as $x*$. This $x*$ should be as close to the original image x.

In this study, we have used an encoder that consists of a convolution layer and a maxpooling layer, while the ReLu activation function is used to normalize the output. The decoder consists of convolution, maxpooling, and upsampling layers. The upsampling layer is a simple layer with no weight that doubles the dimension of the input, while the sigmoid activation function is used in the final layer. Binary cross-entropy is used for the loss function and Adagrad is used as the optimizer.

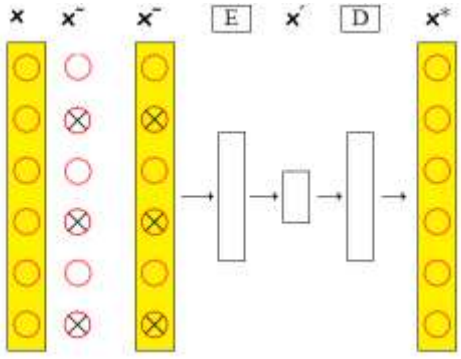

Fig.2. Denoising Autoencoder Workflow

Table.1. Loss Function Values

Input	Loss Function
Noisy	0.036
Reconstructed	0.015

It is expected that only the distorted data will be eliminated. As both the encoder and decoder networks are trained together, the loss function will ensure that the encoder will learn to discard any noise present and maintain only the relevant information, and the decoder will learn to reconstruct an enhanced version of the original input x. Fig.3 shows the effect of the denoising step. Table.1 shows that a smaller value for the loss function is achieved with the reconstructed image.

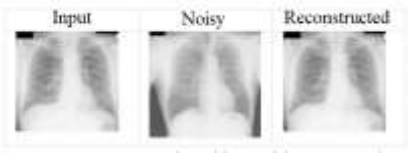

Fig.3. Image Preprocessing with Denoising Autoencoder

3.2 CLAHE

The next preprocessing step, namely Context Limited Adaptive Histogram Equalization (CLAHE), is used to improve the contrast in the images. There are three ideas that drive the CLAHE process: 1) histogram equalization; 2) adaptive histogram equalization; and 3) contrast-limiting.

An image histogram, representing the brightness or tonal value distribution across the picture, is the plot of the number of pixels for each tonal value. The histogram of an image thus provides a visual aid to understand the tonal distribution of the image. Smaller tonal values correspond to the darker areas within a picture and the higher tonal values to the brighter areas. Therefore, the histogram of a dark image will be skewed to the left, while for a bright image, it will be skewed to the right.

Histogram Equalization (HE) is a technique that spreads out the brightness or tonal values to correspond to a flatter, instead of a skewed, histogram, and helps enhance contrast in images. This corresponds to transforming each pixel using a transformation function derived from the tonal values of all pixels, or the entire picture. While this technique enhances the areas of lower local contrast to gain a higher contrast, it does so globally in the picture, which may not be desirable. Thus, a variation of this technique known as Adaptive Histogram Equalization (AHE), addresses this situation by using on each pixel a transformation function derived from a neighbourhood region for that pixel. Another way to describe this technique is that it works with several histograms, each corresponding to a different part of image, and uses these histograms to redistribute the tonal values, helping to improve or enhance contrast locally, instead of globally.

A further improvement over AHE becomes necessary as AHE sometimes might overamplify the contrast in regions where the tonal values remained nearly constant and hence introduce noise amplification. The improvement is achieved through the Contrast-Limited Adaptive Histogram Equalization (CLAHE), by clipping the histogram at a predefined value to limit the amplification. Thus, CLAHE uses two parameters, the Block Size (BS) (or the extent of the local region for local contrast enhancement), and the

Clip Limit (CL) (or the pre-defined tonal value limit for limiting amplification). Increasing the Block Size increases brightness, and increasing the Clip Limit increases the contrast.

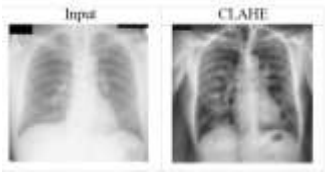

Fig.4. Image Preprocessing by CLAHE

Finally, for implementing CLAHE, each image is divided into sections called tiles, and the histograms of these tiles are equalized, subject to a specified contrast limit. The tiles are put together again using bilinear interpolation. This process helps improve the contrast in the images, as illustrated in Fig.4.

3.3 SEGMENTATION

The purpose of segmentation in image processing is to partition an image into segments or objects so that the pixels in each segment share a common property such as intensity, texture, or color. When segmentation is carried out on CXR images, it greatly helps in the classification of tumors as malignant or benign. For all the segmentation methods used, the indicated threshold is calculated based on the mean and standard deviation. Whatever the segmentation method used, the input is first preprocessed using DAE and CLAHE. As a reference, Fig.5 shows how a sample image is transformed before segmentation is carried out.

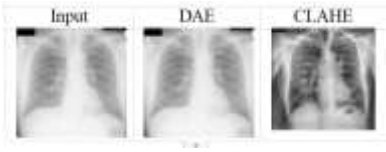

Fig.5. Preprocessing using Both DAE and CLAHE

In this work, we have considered four different segmentation approaches: 1) Canny edge detection with morphology, 2) thresholding with Otsu threshold, 3) automatic thresholding, and 4) granule segmentation with dilation.

3.3.1 Segmentation by Edge Detection:

Developed by Canny [26] in 1986, the Canny edge detector can be used to find a wide range of edges in images. The detection process here consists of three steps. First, a Gaussian filter is used to remove unwanted details and smooth the image. Next, gradient magnitude thresholding is applied to remove any possible erroneous responses to edge detection. Finally, the weak edges are suppressed, and the desired edges are tracked. Once the edges are detected, morphological operations such as dilation and erosion may be applied to further reduce the noise to obtain the segmented image. The Fig.6 shows a sample result of this segmentation.

Fig.6. Canny Edge Detection with Morphology

3.3.2 Otsu Thresholding:

Developed by Otsu [2], the Otsu thresholding method for segmentation determines an optimal threshold value to separate two regions in an image with the maximum inter-class variance. The two classes for our purposes are the foreground and the background based on the grey-scale values of the intensity of the pixels in the image being segmented.

3.3.3 Automatic Thresholding:

Developed by Thamilarasi and Roselin [22] in 2019, the automatic thresholding method used in this study for segmentation determines an optimal threshold value by subtracting a multiple of the standard deviation from the mean for each of the RGB channels.

3.3.4 Segmentation by Granular Computing:

The idea of rough sets, introduced by Pawlak [27] in 1982, forms the basis for granule-based image segmentation. Using the indistinguishability relation, the image is divided into background and object, whose lower and upper approximations are then used to determine the cross-entropy, which is maximized to obtain the threshold to be used for segmentation. A sample of the segmentation results from Otsu threshold, automatic threshold, and granule based segmentation methods is shown in Fig.7.

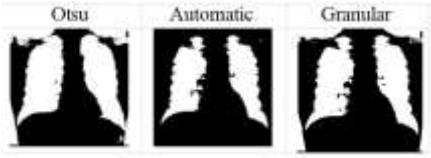

Fig.7. Segmentation by Threshold

3.3.5 Ensemble Segmentation:

The results obtained from the four different segmentation approaches may be aggregated in some manner to come up with an ensemble model for segmentation. The segmentation quality of the ensemble will be influenced by the diversity of the approaches used by the individual approaches. In this study, the ensemble is obtained by scanning the segmented images pixel by pixel. For each pixel, if three or more of the four algorithms define a pixel as a white pixel, then the resultant pixel in the ensemble segmentation will be considered white, and it will be considered black otherwise. A sample segmented image resulting from the ensemble approach is shown in Fig.8, along with the ground truth image.

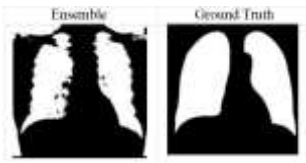

Fig.8. Ensemble Segmented vs Ground Truth Image

The Fig.9 illustrates the outcome from applying the above segmentation methods for a specific image. The performance of each technique is evaluated using the metrics of sensitivity, specificity, accuracy, and dice similarity.

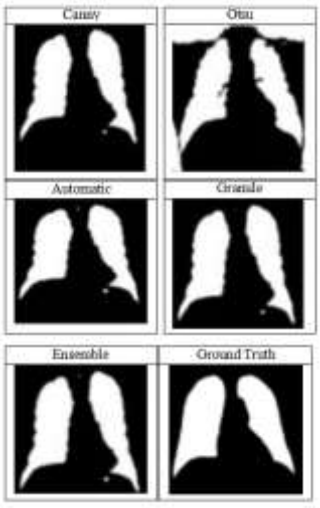

Fig.9. Sample Results from Segmentation Methods Used

3.4 CLASSIFICATION

With accurately segmented images of the lung region, nodule/non-nodule classification and malignant/benign classification can be done more confidently. The classification process entails several steps including feature extraction, feature selection, dimensionality reduction, and feature-based algorithm selection. The main goal of the current study has been segmentation. Therefore, the classification step may be viewed as a validation step for the segmentation process. This is accomplished in two steps, namely feature extraction, and classification. Feature extraction is the most challenging step of extracting the most dominating, appropriate, and correct features from the segmented images that can contribute effectively in the accurate identification of cancerous patients. A suitable method for automatically selecting and classifying the best features is thus required.

- **Feature Extraction and GLCM:** The images segmented using the methods of the previous subsection are subject to feature extraction using the Haralick [28] Gray Level Cooccurrence Matrix (GLCM). The GLCM provides information on the texture of an image by examining cooccurring pixel values in terms of gray-scale values. The features of contrast, correlation, energy, entropy, homogeneity, mean, and standard deviation are extracted from the GLCM.
- **Machine Learning Algorithms Used:** For classification, this study uses the well-known algorithms of Decision Trees (DT), Random Forests (RF), Naive Bayes (NB), Support Vector Machines (SVM), Logistic Regression (LR), K-Nearest Neighbors (KNN), and XGBoost (XGB). The remainder of this subsection is devoted to a brief description of each of these methods.
- **Decision Trees (DT)**: Among the simplest and the most popular methods of machine learning is learning by decision trees. For classification purposes, a decision tree consists of internal nodes that represent conditions on the features, and the decisions resulting from the conditions are represented by the leaf nodes. Classifiers that use Decision trees often lead to overfitting.
- **Random Forests (RF):** The method of random forests is based on the idea of a forest of random trees. It uses multiple decision trees and the idea of feature bagging for classification. It uses the greedy strategy and produces as output the class that is selected by the most number of trees. It corrects the overfitting caused by decision trees and hence outperforms them.
- **Naive Bayes (NB):** The Naive Bayes classifier is a probabilistic classifier that derives from the Bayes theorem. It operates on the premise that the features are pairwise independent and can produce reliable results even with limited amount of data.
- **Support Vector Machines (SVM):** Commonly used for classification and pattern recognition, the method of support vector machines is a supervised learning technique that produces better results compared to query-based searching techniques. This technique accomplishes classification by identifying a decision boundary between the classes.
- **Logistic Regression (LR).** The method of logistic regression produces a discrete or categorical value as the output for a categorical dependent variable. Although this method uses the logistic function and yields only a probability value and does not provide a classification, it is used to build a binary classifier by choosing a cutoff value to indicate one class or another. It can also be generalized to build classifiers of objects falling into multiple classes.
- **K-Nearest Neighbors (KNN).** The foundation of KNN is the idea of similarity points, which are in close proximity to one another. For a specified k, the method classifies an object as belonging to a class that is most among K of its nearest neighbors, using a distance metric such as the Euclidean distance.
- **XGBoost (XGB).** The method of XGBoost, which is an acronym for extreme Gradient Boosting, is an ensemble method which combines gradient descent models to achieve speed and efficiency. It is able to correct errors made by other models by adding new models to the ensemble, controls over fitting, and can handle large datasets with ease.

3.5 FINDINGS FROM THE STUDY

If a segmentation method yields a white pixel in the segmented image corresponding to a white pixel in the ground truth image, then it is considered a true positive, and if the segmentation method yields a black pixel in the segmented image corresponding to a black pixel in the ground truth image, then it is considered a true negative. In a similar manner, a white pixel in the segmented image corresponding to a black pixel in the ground truth image is considered a false positive, and a black pixel in the segmented image corresponding to a white pixel in the ground truth image is considered a false negative. It is customary to demonstrate the robustness of an algorithm as well as to compare two or more algorithms using some common performance metrics. Also, such metrics provide useful information regarding the advantages and limitations of algorithms studied. For segmentation methods, this study has used the metrics of accuracy and dice similarity. The definitions of these metrics are provided in Eq.(1)-Eq.(2) for reference, where TP, TN, FP, and FN denote numbers of True Positives, True Negatives, False Positives, and

False Negatives respectively. All metrics are usually described as percentages.

$$Accuracy = \frac{TP + TN}{TP + FP + TN + FN} \quad (1)$$

$$Dice\,Similarity = \frac{2 \cdot TP}{2 \cdot TP + FP + FN} \quad (2)$$

The study finds that the preprocessing of images using the denoising autoencoder and CLAHE greatly improved the segmentation quality on all the evaluation metrics of performance. The results are summarized in Table.2.

Table.2. Performance of Segmentation Algorithms

Metric Algorithm	Accuracy	Dice Similarity
Canny	94.90	90.91
Otsu	93.98	88.93
Automatic	94.89	91.03
Granule	95.93	92.70
Ensemble	97.67	94.41

Table.3. Classification Accuracies

Accuracy of Algorithms	Nodule/ Non-nodule	Malignant/ Benign
Random Forests	95.60	96.81
Decision Trees	93.98	94.11
Naive Bayes	96.89	97.76
SVM	98.93	99.18
Logistic Regression	96.67	98.74
KNN	97.90	98.14
XGBoost	93.98	97.34

Another instrument that is often used to validate the quality of binary classifiers is the Receiver Operating Characteristic (ROC) curve, which is the plot of sensitivity or the true positive rate (TPR) on the y-axis against 1-specificity on the x-axis, where specificity is also known as the true negative rate (TNR) as obtained by varying the threshold value used for classification. Note that 1 − TNR is also characterized as the false positive rate (FPR). In terms of TP, FP, TN and FN, the quantities TPR and TNR are defined by Eq.(3)- Eq. (4).

$$Sensitivity\left(TPR\right) = \frac{TP}{TP + FN} \quad (3)$$

Table.4.Sensitivity (TPR) and 1-Specificity (FPR)

RF		KNN		SVM	
TPR	**FPR**	**TPR**	**FPR**	**TPR**	**FPR**
0.15	0.01	0.00	0.00	0.01	0.01
0.22	0.02	0.71	0.00	0.44	0.04
0.32	0.05	0.76	0.00	0.67	0.11
0.41	0.03	0.80	0.00	0.68	0.28
0.54	0.05	0.82	0.00	0.75	0.30
0.64	0.05	0.85	0.01	0.80	0.59
0.70	0.10	0.91	0.07	0.90	0.65
0.89	0.21	0.97	0.20	0.97	0.79
0.97	0.65	0.99	0.45	0.99	0.90
0.98	0.86	1.00	1.00	1.00	0.97

Some representative values of TPR and FPR obtained from some of the classification algorithms in the present study are shown in Table.4. A visualization of this data is shown as ROC curves in Fig.12. The fact that all of the ROC curves are skewed significantly to the left indicates that our segmentation approach is able to yield superior classification accuracy. Also, it is emphasized that the Area Under the ROC Curve (AUC) for all algorithms used in the study are close to 1.0, which validates the classification quality even more.

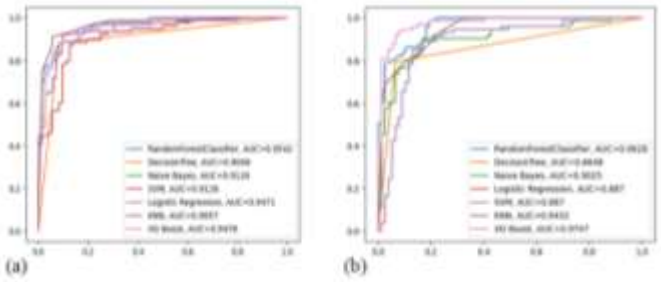

Nodule vs. Non-nodule classification (b) Malignant vs. Benign classification

Fig.12. ROC for CXR Classification

Comparison of this improved accuracy of enhanced ensemble segmentation with existing experiment [25] as follows. This results shows that enhanced ensemble segmentation achieved higher accuracy than existing one.

Table.5. Comparison with existing method

Segmentation Models	Accuracy
Ensemble segmentation	97.67
Proposed Ensemble segmentation	92.02

Above Fig.shows the Comparison of proposed and existing methods and the proposed model is achieves higher accuracy than existing models

Table 6. Evaluation of proposed model

Metrics	Value
Sensitivity	69.4646
Specificity	98.52967
Accuracy	92.0252
DC	79.20411

The above table depicts the overall performance of the proposed model. The values of accuracy and specificity shows that proposed model attained balanced classification, and which is better than previous discussed experiments.

4. CONCLUSION

This study has explored several methods for segmentation and classification lung CXR images. The preprocessing of images with a denoising Autoencoder and CLAHE greatly improves the performances of segmentation and classification. The segmentation approaches explored include Canny edge/morphology segmentation, Otsu threshold segmentation, automatic threshold segmentation, and granule segmentation. Additionally, an ensemble of all the above segmentation methods has been studied as well. The ensemble approach yields the highest segmentation accuracy of 97.67%. Using the GLCM to extract features from the segmented images, the study has included the machine learning algorithms of Random Forests, Decision Trees, Naive Bayes, SVM, Logistic Regression, KNN, and XGBoost. The accuracy achieved for nodule/nonnodule classification peaked at 98.93% with SVM. The highest accuracy of 99.18% was achieved for malignant/benign classification with SVM as well. For CXR images, from this study it appears like ensemble segmentation and SVM classification are most suited for segmentation and classification respectively. The nature of the ROC curves obtained for the various classification algorithms clearly validates the effectiveness of the ensemble approach used for segmentation. This research concluded that results were improved by preprocessing techniques and influence the results of segmentation and classification.

REFERENCES

[1] A. Priya, R.K. Agrawal and B. Rana "Fusion-based Multilevel Thresholding for Image Segmentation using Evolutionary Algorithm", *Proceedings of International Conference on Electrical, Electronics and Computer Engineering*, pp. 1-7, 2022.

[2] N. Otsu, "A Threshold Selection Method from Gray-Level Histograms", *IEEE Transactions on Systems, Man and Cybernetics*, Vol. 9, No. 1, pp. 62-66, 1979.

[3] A. Tsallis, A. Rajagopal, I. Plastino, J. Andricioaei S. Stranb and J. Abe Klos, "Nonextensive Statistical Mechanics and Its Applications", 2001.

[4] J.N. Kapur, P.K. Sahoo and A.K. Wong, "A New Method for Gray-Level Picture Thresholding using the Entropy of the Histogram", *Computer Vision, Graphics and Image Processing*, Vol. 29, No. 3, pp. 273-285, 1985.

[5] K. Ramesh, G.K. Kumar, K. Swapna, D. Datta and S.S. Rajest, "A Review of Medical Image Segmentation Algorithms", *EAI Endorsed Transactions on Pervasive Health and Technology*, Vol. 7, No. 27, pp. 1-7, 2021.

[6] G. Liu, Z. Zhang, X. Cui, J. Kuang, J. Cai and X. Ji, "Chromosome Image Segmentation based on OTSU and Region Growing Algorithm", *Proceedings of International Conference on Pattern Recognition and Artificial Intelligence*, pp. 1046-1050, 2022.

[7] L. Fang, "Research on Image Fuzzy Threshold Segmentation Algorithm based on Fuzzy Theory", *Proceedings of International Conference on Information Technology, Big Data and Artificial Intelligence*, Vol. 2, pp. 94-97, 2021.

[8] X. Xinying, Z. Zhijun, X. Jun and X. Keming, "Threshold Image Segmentation based on Granular Immune Algorithm", *Chinese Control and Decision Conference*, pp. 3512-3515, 2009.

[9] P.S. Liao, T.S. Chen and P.C. Chung, "A Fast Algorithm for Multilevel Thresholding", *Journal of Information Science and Engineering*, Vol. 17, No. 5, pp. 713-727, 2001.

[10] C. He, X. Wang, L. Deng and G. Xu, "Image Threshold Segmentation based on GLLE Histogram", Proceedings of International Conference on Internet of Things and IEEE Green Computing and Communications and IEEE Cyber, Physical and Social Computing and IEEE Smart Data, pp. 410-415, 2019.

[11] A. Renyi, "On Measures of Entropy and Information", *Proceedings of Berkeley Symposium on Mathematical Statistics and Probability*, Vol. 4, pp. 547-562, 1961.

[12] F.Nie, P. Zhang, J. Li and D. Ding, "A Novel Generalized Entropy and its Application in Image Thresholding", *Signal Processing*, Vol. 134, pp. 23-34, 2017.

[13] S.S. Raoof, M.A. Jabbar and S.A. Fathima, "Lung Cancer Prediction using Machine Learning: A Comprehensive Approach", *Proceedings of International Conference on Innovative Mechanisms for Industry Applications*, pp. 108-115, 2020.

[14] H. Sarker, "Machine Learning: Algorithms, Real-World Applications and Research Directions", *SN Computer Science*, Vol. 2, pp. 1-7, 2021.

[15] A. Pratondo, C.K. Chui and S.H. Ong, "Integrating Machine Learning with Region-based Active Contour Models in Medical Image Segmentation", *Journal of Visual Communication and Image Representation*, Vol. 43, pp. 1-9, 2017.

[16] R. Cohen, "The Chan-Vese Algorithm", *Computer Vision and Pattern Recognition*, pp. 1-18, 2011.

[17] D. Wang, J. Mo, G. Zhou, L. Xu and Y. Liu, "An Efficient Mixture of Deep and Machine Learning Models for COVID-19 Diagnosis in Chest X-ray Images", *PloS One*, Vol. 15, No. 11, pp. 1-9, 2020.

[18] A. Khan, R. Garner, M.L. Rocca, S. Salehi and D. Duncan, "A Novel Threshold-based Segmentation Method for Quantification of COVID-19 Lung Abnormalities", *Signal, Image and Video Processing*, pp. 1-8, 2022.

[19] R. Muhamedyev, K. Yakunin, S. Iskakov, S. Sainova, A. Abdilmanova and Y. Kuchin, "Comparative Analysis of Classification Algorithms", *Proceedings of International Conference on Application of Information and Communication Technologies*, pp. 96-101, 2015.

[20] D. Savchuk and A. Doroshenko, "Investigation of Machine Learning Classification Methods Effectiveness", *Proceedings of International Conference on Computer Sciences and Information Technologies*, Vol. 1, pp. 33-37, 2021.

[21] A.O. Salau and S. Jain, "Feature Extraction: A Survey of the Types, Techniques, Applications", *Proceedings of International Conference on Signal Processing and Communication*, pp. 158-164, 2019.

[22] V. Thamilarasi and R. Roselin, "Automatic Thresholding for Segmentation in Chest X-Ray Images based on Green Channel using Mean and Standard Deviation", *International Journal of Innovative Technology and Exploring Engineering*, Vol. 8, No. 8, pp. 695-699, 2019.

[23] V. Thamilarasi and R. Roselin, "Survey on Lung Segmentation in Chest X-Ray Images", *The International*

Journal of Analytical and Experimental Modal Analysis, pp. 1-9, 2019.

[24] V. Thamilarasi and R. Roselin, "Lung Segmentation in Chest X-Ray Images Using Canny with Morphology and Thresholding Techniques", *International Journal of Advance and Innovative Research*, Vol. 6, No. 1, pp. 1-7, 2019.

[25] V. Thamilarasi and R. Roselin, "Granule based segmentation using Rough Entropy and Classification in Chest X-ray image", *Proceedings of International Conference on Computational Science and Intelligence*", pp. 35-49, 2020.

[26] J. Canny, "A Computational Approach to Edge Detection", *IEEE Transactions on Pattern Analysis and Machine Intelligence*, Vol. 8, No. 6, pp. 679-698, 1986.

[27] Z. Pawlak, "Rough Sets", International Journal of Computer and Information Sciences, Vol. 11, pp. 341-356, 1982.

[28] R.M. Haralick, K. Shanmugam and I.H. Dinstein, "Textural features for image classification", *IEEE Transactions on Systems, Man and Cybernetics*, Vol. 3, No. 6, pp. 610-621, 1973.